

STATUS OF ADVANCED TURBOPROP TECHNOLOGY

J. F. Dugan, B. A. Miller, and D. A. Sagerser
Lewis Research Center

SUMMARY

When used to power medium-range transport aircraft cruising at Mach 0.8, advanced turboprops offer a 10 to 20 percent fuel saving relative to advanced turbofans and a 5 to 10 percent DOC advantage with .15.8¢/liters (60¢/gallon) fuel. Because of this attractive potential, NASA began the Advanced Turboprop Program in fiscal year 1978 as the sixth major part of its Aircraft Energy Efficiency Program. In the two previous fiscal years, NASA supported, as part of its R&T base program, some turboprop-powered transport studies, some wind tunnel aerodynamic and acoustics tests of model propellers (0.62 m in diameter), a study of turboprop maintenance, and an experimental wind-tunnel program on airframe-turboprop interactions. This paper reviews each of these areas and describes plans for continued development of the technology for advanced turboprop transport aircraft.

INTRODUCTION

The Advanced Turboprop Program is one of six major technology programs that compose the NASA Aircraft Energy Efficiency Program (ref. 1). It is intended to demonstrate the technology readiness for efficient, reliable, and acceptable operation of turboprop-powered commercial transports at cruise speeds up to Mach 0.8 and at altitudes above 9.144 km (30 000 ft). This technology would also apply to possible new military aircraft requiring long-range and long-endurance subsonic capability.

The Advanced Turboprop Program grew out of studies of low-energy-consumption aircraft engines. These studies, which ran from 1974 to 1976, were conducted, under contract to Lewis, by General Electric (refs. 2 and 3) and Pratt & Whitney Aircraft (refs. 4 and 5). The objectives of these studies were to identify and evaluate ways to reduce fuel consumption in current and future subsonic transport engines. Among the conclusions was this: The most promising unconventional engine concept is an advanced turboprop, which may permit a 15- to 20-percent fuel saving compared with the projected fuel usage of an advanced turbofan engine. This conclusion prompted, in late 1975, NASA R&T studies of high-speed propellers (the High-Speed Propeller Technology program). By 1977 enough progress had been made in propeller technology to justify the start of phase I of the Advanced Turboprop Program. The planning of the Advanced Turboprop Program and the status of research in advanced turboprops as of July 1977 are discussed in reference 6.

This paper, an update of reference 6, reviews results obtained since July 1977. It includes propeller efficiency data from three sets of propeller

blades tested in the Lewis 8- by 6-foot wind tunnel, propeller-wing interaction drag obtained in the Ames Research Center 14-foot wind tunnel using a propeller slipstream simulator, final cost figures from a study of turboprop-system reliability and maintenance costs, and recent estimates of fuel savings and direct-operating-cost (DOC) savings for turboprop-powered transports compared with projected fuel usage and cost for turbofan-powered transports.

MAJOR AREAS OF ADVANCED TURBOPROP PROGRAM

The four major areas involved in the Advanced Turboprop Program - the propeller and nacelle, cabin environment, installation aerodynamics, and mechanical components - are shown in figure 1. These areas interact, and all contributed to the program goals of low fuel consumption, low operating cost, and passenger acceptance.

The propeller and its nacelle must be designed to achieve high efficiency for cruise at speeds up to Mach 0.8 above 9.144 km (30 000 ft). The propeller blades will be very thin and have swept leading edges in order to minimize compressibility losses. The spinner and nacelle will be shaped to minimize choking and compressibility losses, especially near the blade roots. The successful application of these concepts will result in higher propeller efficiencies. This, of course, will contribute to both low fuel consumption and low operating cost, since fuel accounts for such a large fraction of operating cost.

In a later section, Propeller Efficiency, the propeller data obtained from three sets of blades tested in the Lewis 8- by 6-Foot Wind Tunnel will be discussed; the plans for testing four more sets of blades before selecting the propeller design for large-scale propeller development in phase II of the Advanced Turboprop Program will also be discussed.

The sketch at the lower right of figure 1 labeled "cabin environment" reminds us that the fuselage is in the direct noise field of the propeller (whereas the inlet duct of a turbofan shields the fuselage from fan noise). The propeller tips may be slightly supersonic at the Mach 0.8 cruise condition, resulting in a relatively high noise level. The noise level must be attenuated by the cabin wall in order to provide a quiet cabin environment. Since it is likely that additional airframe weight will be needed to achieve the required attenuation, the quiet cabin environment is achieved at the expense of fuel economy and operating cost. Just how much is not known at this time.

Included in the section Propeller Noise and Fuselage Attenuation will be a discussion of early noise data obtained by simulating Mach 0.8 cruise conditions, plans to obtain more reliable noise data in flight at Mach 0.8, and a brief description of three fuselage structural concepts proposed for attenuating propeller noise.

At the lower left of figure 1 the sketch labeled "installation aerodynamics" depicts an accelerated, swirling propeller slipstream flowing over a wing. Here, there is a potential for higher drag which would adversely affect

fuel consumption and operating cost. The increased Mach number of the flow over the wing segments washed by the propeller slipstream and the flow rotation in the propeller slipstream may cause large interference drag penalties in cruise. On the other hand, there is the possibility that fuel consumption and operating cost can be improved by special tailoring of the wing segments washed by the propeller slipstream. The magnitude of swirl in the propeller slipstream results in very substantial losses in propeller efficiency which are attributed to the swirl component of slipstream momentum. A properly designed wing in the slipstream can be expected to straighten the flow and to experience a corresponding thrust force. This resulting thrust force may offset or even exceed the drag penalties due to propulsion system/airframe interference. Because of the complexity of the aerodynamic processes involved, detailed wind-tunnel testing and analysis will be required to provide reliable answers.

These planned experimental and analytical programs are discussed in the Airframe-Propulsion System Integration section; also discussed are some early experimental results obtained using a slipstream simulator.

The sketch in the upper left shows the mechanical components of an advanced turboprop propulsion system. Two of the components are singled out as being especially important in achieving a low operating cost: the advanced propeller and its gearbox. For maximum direct operating cost advantage, their maintenance costs must be lower than the costs of earlier-design commercial turboprop aircraft. The final results from a study of turboprop-system reliability and maintenance costs are discussed in the Propeller and Gearbox Maintenance section.

The most recent assessment of the fuel savings and the DOC savings of turboprop-powered transports is discussed in the section Advanced Turboprop Aircraft Studies.

Propeller Efficiency

One aspect of the advanced turboprop system performance that required early experimental verification was the propeller aerodynamic efficiency. Test results were needed to demonstrate that high efficiency at high cruise speeds could be obtained with advanced propeller designs that use thin blade sections. Three propeller models (62.23-cm (24.5-in.) in diam.) have been designed and are being tested in a wind tunnel to measure their performances. Two of the models, designated SR-1 and SR-2, were first tested by Hamilton Standard (under NASA contract) in a wind tunnel at United Technologies Research Center (UTRC; refs. 7 and 8). These two and a third model, SR-1M, are now being tested in a wind tunnel at Lewis. Propeller model SR-1 is shown installed on the propeller test rig in the Lewis 8- by 6-foot wind tunnel in figure 2.

All three models have eight blades and were designed to operate at a cruise speed of Mach 0.8, a tip speed of 244 m/sec (800 ft/sec), and a disk loading of 301 kW/m² (37.5 shp/ft²) at an altitude of 10.67 km (35 000 ft). Two of the models, SR-1 and SR-1M, were designed with 30° of aerodynamic sweep at the blade tips, and the third, SR-2, has straight blades. Both the SR-1 and

SR-1M models incorporated conical spinners, and the SR-2 model incorporated an area ruled spinner that was designed to lower flow velocities in the hub region where choking could be a problem.

Model SR-1M is actually a modification to the SR-1 design and differs primarily in the blade twist and camber distribution from hub to tip. This model was created when the results of initial wind tunnel tests at the UTRC showed that the radial loading differed from the design distribution and the efficiency was somewhat lower than predicted. The changes incorporated in model SR-1M were designed to increase the loading in the outboard region of the blade to conform more closely to the initial objective.

Predicted and measured efficiencies for the three models are tabulated in table I. The values shown are at the design loading and tip speed of 301 kW/m^2 (37.5 shp/ft^2) and 244 m/sec (800 ft/sec), respectively, which results in a C_p of 1.7 and a J of 3.06. The current prediction design-point efficiency of SR-1 is over 2 percent higher than that of SR-2. This reflects the anticipated benefit of the 30° of blade sweep. However, when these models were tested, their measured efficiencies were about the same and were close to the predicted value for SR-2. Because the slightly higher than predicted performance for SR-2 may be associated with the area-ruled spinner used on this model, further tests of this spinner configuration are planned.

Tests of model SR-1M showed that the modifications made to the blade twist and camber distributions did not improve the design point efficiency even though recent radial wake survey measurements made downstream of the blades indicated that the intended radial loading distribution had been achieved and no gross flow problems occurred. At lower Mach numbers, however, model SR-1M performed significantly better than models SR-1 and SR-2. For example, at Mach 0.7 SR-1M's 81.7 percent efficiency was about 1.5 percent better than either SR-1 or SR-2. The value of 81.7 percent is within 4 percent of the ideal induced efficiency (inviscid) limit of 85.1 percent and thus is about as high as can be practicably achieved for a thin bladed propeller operating without compressibility losses.

The results obtained from the models tested so far suggest that the lower than predicted efficiencies at design conditions may have resulted from higher than anticipated compressibility losses. This, in turn, suggests that performance at the higher cruise speeds may be improved by the use of additional blade sweep.

It is appropriate at this point to compare the model test results with the efficiency goal of 80 percent, a value assumed in the initial RECAT studies references 9 to 13. This is done for model SR-1M in figure 3 - a plot showing the effect of cruise Mach number and loading on efficiency. The SR-1M test data used in this figure differ somewhat from data shown in table I in that the blade angle and tip speed were chosen for maximum efficiency at the specified value of loading rather than holding the design value for J and thus fixing tip speed. It should also be noted that the power loading (power/diameter² or P/D^2) varied with the cruise velocity cubed by maintaining constant values for C_p/J^3 . Such a variation approximately matches the thrust levels required by a family

of similarly sized aircraft, each designed for different cruise speeds.

At the design cruise speed of Mach 0.8 and 100 percent loading, the measured efficiency for model SR-1M was less than 3 percent below the goal. By reducing the loading to somewhat less than 70 percent of design (and thus increasing the propeller tip diameter a little over 20 percent) the efficiency goal of 80 percent can be obtained. This efficiency can also be reached at 100 percent loading by lowering the cruise speed to slightly less than Mach 0.75 or by some combination of reduced loading and reduced cruise speed. Reducing cruise speed or loading also has the effect of reducing the maximum efficiency tip speed, and lower tip speeds result in lower noise levels.

Thus, while current propeller models have not demonstrated the 80 percent efficiency goal at design conditions, performance at this level has been demonstrated at reduced loading or reduced cruise speeds. Improvements continue to be made in propeller aerodynamic design methodology based on new test results and analysis. Performance improvements are expected to result from additional blade sweep, improved area ruling in the hub, and a better understanding of the propeller flow field through improved flow survey testing. These improvements are expected to result in obtaining the 80 percent efficiency goal at design loading and Mach number.

A new propeller model, designated SR-3, is currently being fabricated for wind-tunnel tests in April and May of this year. This model is the first to be designed with acoustic considerations. Its plan form and significant design characteristics are compared with models SR-1, SR-1M, and SR-2 in figure 4. The tip speed, loading, and number of blades are the same for all of these models. But the tip sweep angle was increased to 45° for model SR-3 because of the expected aerodynamic and acoustic benefits. Because of this and other refinements in the blade design procedures and spinner area ruling, the estimated design efficiency is 2 percent higher, and the estimated design cruise noise level is 6 dB lower than the SR-1 and 1M designs.

NASA's current propeller model test program is diagramed in figure 5. Four propeller design approaches, in terms of cruise Mach number, tip speed, loading, and number of blades, are included in the model program so that the trade-offs among the more important propeller design parameters may be evaluated.

The first approach assumes an 0.8 cruise Mach number, eight blades, a 244-m/sec (800-ft/sec) tip speed, and a 301-kW/m² (37.5-hp/ft²) disk loading. Three models, SR-1, SR-2, and SR-1M, have been designed, built, and are being tested to determine their performance and noise characteristics. A fourth model, SR-3, has been designed, is being built, and will be tested to determine the effect of additional sweep and improvements in design methodology. A fifth model in this category, SR-4, will be used to evaluate the benefit of advanced airfoils on performance.

Because propeller noise level requirements are, at present, uncertain, two lower-tip-speeds-design approaches are planned. Both will have 10 blades and

lower disk loadings (larger tip diameters) to maintain high efficiency at the lower tip speeds. The 213-m/sec (700-ft/sec) tip-speed SR-6 model is expected to have an efficiency about the same as SR-3. And the 183-m/sec (600-ft/sec) tip speed SR-5 model is expected to have a slightly lower efficiency than SR-3, but SR-5's tip relative Mach number is just sonic and therefore much lower noise levels are expected.

A final design approach, which assumes a 0.7 cruise Mach number, is included in the plan to assess the benefits of lower cruise speeds on propeller design. The design of this model will be compared with an 0.8 cruise Mach number design to determine if there is enough difference in the resulting blade shape and predicted performance to justify fabrication and test. If not, the test results of a 0.8 Mach number design operating off-design down to Mach 0.7 will be used to assess the effect of lower cruise speed on propeller design performance.

The test results from the propeller models representing each design approach will be used with results from other tests and design studies affecting the propeller design to define a system-optimized design, designated SR-7. The other studies include the development of improved aerodynamic and acoustic design tools, studies of full-size blade structural designs, aeroelastic model tests, fuselage noise attenuation design studies, and aircraft system studies. A model of the SR-7 design will be tested to verify predicted performance. Then, a full scale model of this design, or a modification of it, will be built and flight tested as part of phase II of the program.

PROPELLER NOISE AND FUSELAGE ATTENUATION

Propeller Noise

For an advanced turboprop aircraft to be competitive with an advanced turboprop aircraft, the turboprop cabin interior during cruise should be equivalent in comfort (low levels of noise and vibration) to that of the turboprop aircraft. However, quiet cabin interior will be more difficult to achieve in the turboprop aircraft because its fuselage is in the direct noise field of the propeller (whereas the inlet duct of a turboprop shields the fuselage from fan noise).

Some preliminary noise tests of SR-1 and SR-2 were completed in 1976 in the UTRC Acoustic Research Tunnel (fig. 6). To simulate Mach 0.8 cruise operation, the tunnel was operated at its maximum through-flow Mach number (Mach 0.32), and the propeller model was oversped so that the blade tip relative Mach number was the same as for the Mach 0.8 cruise condition. The propeller model had only two blades in these tests because of the limited horsepower of the electric drive rig. Microphones were located on a line parallel to the propeller axis of rotation at three radial distances in the near field and one radial distance in the far field. Measured noise levels in the tunnel were compared with levels predicted by a theoretically based computer program. Empirical adjustments were made to the noise prediction program, which was then used to predict full-scale propeller noise at the desired altitude and cruise conditions. The overall near-field sound pressure level (SPL) of SR-1 and SR-2 at

Mach 0.8 cruise is 146 ± 3 dB. The 6-dB uncertainty band is a result of imperfections in the testing technique and the prediction program.

With the intent of acquiring better propeller noise data at Mach 0.8 cruise conditions, two feasibility studies were conducted: one of a high-speed wind tunnel and the other of flight tests (fig. 7). For the flight tests the 0.61-m (2-ft) diameter propeller model would be mounted above the fuselage of a JetStar aircraft, and the fuselage instrumented with microphones. The flight tests would yield high quality acoustic data with respect to noise level, spectral content, and directionality. Data obtained from the high-speed wind tunnel, however, would be uncertain with respect to both level and directionality. Such an uncertainty in the tunnel data is extremely difficult to quantify without comparison with flight data. Thus a decision was made to proceed with the flight tests.

Fuselage Attenuation

The noise perceived by the passenger inside the cabin is a strong function not only of the noise generated by the propellers, but also of the noise attenuated by the fuselage and interior cabin construction. The present state of affairs is illustrated in figure 8. The desired cabin noise level is assumed to be 75 dB A. Assuming the cabin noise to be dominated by the blade passing frequency tone at 160 Hz, the sound pressure level would be 90 dB inside the cabin. An aircraft with a conventional fuselage and wing-mounted turboprops could tolerate a propeller noise level outside the cabin of about 110 dB.

Now, consider the propeller noise level estimated from the 1976 tests of SR-1 and -2; that is, 146 ± 3 dB. By tailoring the sweep and planform of the SR-3 blades for lower noise, a sound pressure level of about 140 dB is predicted. A further reduction to about 135 dB might be achieved by using new low-noise airfoils. That is probably the lower limit of propeller noise for the design parameters noted (eight blades; tip speed, 244 m/sec (800 ft/sec); power loading, 301 kW/m^2 (37.5 hp/ft^2)).

However, a 135-dB propeller noise level is about 45 dB above the desired cabin noise level and about 25 dB above the noise level that can be attenuated with conventional fuselage construction. Four ways of bridging this 25-dB gap have been suggested: (1) Design propeller tip speed could be reduced to lower the noise generated by the propeller. (2) Fuselage design and cabin acoustic treatment can almost certainly be improved using conventional techniques to increase noise attenuation. (3) The propeller and fuselage design can be integrated, particularly in the selection of propeller blade passing frequency and fuselage acoustic modes. This is expected to produce even greater improvement in propeller noise attenuation. (4) Finally, the engine location on the aircraft can be optimized; for example, mounting the engines farther outboard on the wing or on the aft end of the fuselage behind the passenger cabin would result in less cabin noise.

Three quite different fuselage structural concepts for attenuating propeller noise are illustrated in figure 9. A conventional fuselage attenuates noise generated at different frequencies as shown in figure 9(a). The least attenuation occurs in the frequency range of several hundred hertz. Unfortunately, the blade passing frequency of many propeller designs falls in this range. Three concepts have been suggested to resolve this problem:

(1) One concept involves structural tuning and damping (fig. 9(b)) wherein the structure is designed to couple in preferred modes of vibration the acoustic energy that can then be effectively reduced by damping material. When only discrete tones are the source of excitation, the structure can be tuned to have much reduced response at those frequencies. This concept is currently in a state of analytical development, although some encouraging experimental results have been obtained. For this reason only very general trends of noise reduction and attendant weights of fuselage structure change are available.

(2) The increased stiffness approach to attenuating propeller noise is shown in figure 9(c). High stiffness is achieved by fastening aluminum skin to closely spaced aluminum and graphite-epoxy frames. This concept is more effective at lower propeller blade frequencies. Thus, lower propeller tip speed and fewer blades enhance propeller noise attenuation. (Of course, lowering propeller tip speed is also a way to reduce the noise generated by the propeller.)

(3) The double limp wall concept (fig. 9(d)) is more effective at the higher propeller blade frequencies. Attenuation improves as propeller tip speed increases, but then, so does propeller noise generation. The double limp wall concept also is in the development stage. It may, for example, be necessary to increase the number of propeller blades in order to raise the blade passage frequency to a value that will allow the fuselage wall to exhibit mass-like behavior. Also, structural damping may be required in order to approximate mass-like response.

It is quite possible that an optimized fuselage acoustic design will selectively employ portions of all three concepts to obtain maximum noise reduction with minimum weight penalty.

AIRFRAME-PROPULSION SYSTEM INTEGRATION

The initial systems studies (refs. 9 to 15) identified the integration of the turboprop propulsion system with the airframe as one of the areas of high uncertainty that requires additional research. The integration of a turboprop is more critical than that of a turbofan because of the large interaction between the slipstream and wing. As outlined in the studies, the combination of a supercritical swept wing and the highly loaded propeller can give rise to a considerable level of aerodynamic interference. Inherent in the slipstream are Mach number and swirl increments of approximately 0.05 and 6.0° , respectively. Both of these flow perturbations can significantly affect the flow over a supercritical wing which has been designed to operate at a specific Mach number. Either can cause the section of the wing within the slipstream to operate

well into drag-rise, effectively reducing the installed performance of the propeller. In addition, the propeller will be subject to a nonuniform flow field created by the airframe, thus potentially reducing its performance.

To reduce the uncertainties associated with the installation of these advanced turboprop propulsion systems, a combined experimental and analytical research program has been initiated. The primary objectives, as enumerated in figure 10, are to assess the magnitude of the aerodynamic interference, to understand the aerodynamic phenomena associated with the installation, and to develop an analytical and experimental data base. The data base will be acquired using a slipstream simulator and a powered semispan model. The determination of the aerodynamic interference between the propulsion system and airframe will significantly contribute to the technology required to establish the overall performance potential of the proposed high-speed turboprop aircraft. The design and optimization of the propulsion system installation requires a detailed understanding of the aerodynamic and flow characteristics associated with this type of installation. The development of the analytical and experimental data base will contribute to this understanding.

Experimental Program

Current experimental programs for the near future include two complementary test programs: the first uses a simulated propeller slipstream, and the second, an active propeller.

The slipstream simulator program (fig. 11) provided fundamental force and pressure data on the interaction of a representative slipstream and a supercritical wing. The slipstream was generated using an ejector-driven nacelle strut mounted in front of a transonic wing-body model. The ejector-drive nacelle was powered by 20 sets of ejector nozzles which controlled the energy and hence the velocity of the slipstream. The nacelle also included a set of swirl vanes to induce swirl into the slipstream. The wing-body model was mounted on a force balance and the wing was pressure instrumented. With this arrangement, the effects of slipstream Mach number and swirl on the wing-body forces and pressure were determined. To provide a more detailed understanding of the interaction between the slipstream and wing, a wake rake was used to measure the wake characteristics along the span of the wing. This information provided a detailed description of the local drag characteristics along the wing and identified the local drag increments resulting from the slipstream-wing interaction. The slipstream simulator test program was conducted in the latter part of fiscal year 1977 in the Ames Research Center 14-foot wind tunnel. The results are shown in figure 11. For all test points the slipstream Mach number was higher than the cruise Mach number by 0.075. With zero swirl in the simulated slipstream, aircraft drag increased about 2.5 percent. Theory predicts that, as swirl increases in the slipstream, aircraft drag will decrease. The experimental data bear this out, except for an anomaly at a 6° swirl. The reason for this is not yet known. These preliminary results show that the drag penalties associated with the interaction of a turboprop slipstream and a supercritical wing are not excessive and that the potential does exist to recover some of the propeller swirl losses with the wing.

The second, or active propeller program will provide a more accurate estimate of the interference between the propulsion system and the airframe, including the effects of the installation on the actual propeller performance. This test program, which will be conducted in the Ames 11- by 11-foot wind tunnel during the first half of fiscal year 1979, will use an active propeller mounted on a semispan wing-body model. To insure consistency between these results and those of the isolated propeller tests, the propeller blades of the two test programs are the same aerodynamic design. Furthermore, the semispan wing-body model is a scaled version of the full-span model used with the slipstream simulator. This will allow a detailed comparison with the slipstream simulator data. The propeller on the semispan model will be powered by an air turbine motor and be instrumented for propeller thrust and power measurements. The wing-nacelle combination will be mounted on a floor balance and be instrumented for pressure measurements.

The slipstream simulator tests and the active propeller tests complement each other. The slipstream simulator tests, although providing only an approximate simulation in terms of slipstream Mach number and swirl, does allow the individual interactions to be investigated separately and in combination. Because of the necessity of maintaining the alignment between the ejector nacelle and the free-stream flow direction, only measurements corresponding to the conditions around the cruise angle of attack can be obtained. However, the relative position of the slipstream and wing can be easily varied. In contrast, the active propeller program provides an accurate and complete simulation of the flow field over the full angle-of-attack range. However, it is more difficult to identify the effects of the various flow perturbations and to vary them to establish trends that can be used to optimize the installation. Jointly though, these two test programs should provide a detailed understanding of the various interference effects and establish an accurate assessment of installed performance of these high-speed turboprops.

Analytical Program

To provide an analytical base for the integration of these advanced turboprop propulsion systems, two approaches are being pursued: The first is to apply existing linear paneling techniques to the wing-nacelle-slipstream combination as described in reference 16. Although these techniques are applicable only subcritically, it is believed that many of the potential transonic flow problems can be identified by examining the local pressure distributions at subcritical conditions. Several paneling techniques are being applied to this area and include those described in references 16 to 18. The accuracy of these methods will be evaluated using the experimental results obtained from the test programs. The second, a long-range analytical effort, is to develop a transonic computational technique capable of analyzing a wing-nacelle-slipstream combination under transonic flow conditions.

PROPELLER AND GEARBOX MAINTENANCE

A study of turboprop system reliability and maintenance costs was completed in May 1977 by Detroit Diesel Allison (DDA) for Lewis. The objectives of the study were to determine the overall reliability and maintenance costs (R&MC's) of past and current turboprop systems and then to project the R&MC improvements that could be expected for new turboprop systems for the 1985-1990 IOC. Hamilton Standard (HS) was a subcontractor to DDA and provided information on past, current, and new propellers. The aircraft studied were the Lockheed L188 Electra, Convair CV580, and Lockheed L382 Hercules. These aircraft were powered by the DDA 501-D13 turboshaft engine and either the DDA 606 propeller or the HS 54H60 propeller. The data used in the study were obtained from airline records, outside repair facilities, CAB Form 41, and the DDA reliability department records.

The fully burdened turboprop maintenance cost was quite high. Using data from 1966 through 1969 for Electra L188 operations averaging 0.80 hour per flight, the turboprop (DDA 501-D13/HS 54H60) maintenance cost was \$42.30 per flight hour (FH) (in CY 1976 dollars).

In figure 12 the high maintenance cost of the DDA/HS turboprop is compared with the maintenance cost of the JT8D turbofan that powered B-737 aircraft from 1971 to 1973. The higher turboprop maintenance cost (\$53.18/FH) resulted from scaling the turboprop so that its thrust capability equaled that of the JT8D turbofan at Mach 0.8 and 10.67 km (35 000 ft) altitude. In this comparison, the turboprop maintenance cost exceeds the turbofan maintenance cost by \$22.71 per engine flight hour or by 74.5 percent. However, most of the difference (\$18.13) was due to the higher maintenance cost of the older technology turboprop core. The small remaining difference (\$4.58) comes from the higher maintenance cost of the turboprop's propeller and gearbox compared with the turbofan's fan and thrust reverser. For future systems it can be assumed that the maintenance cost of the core will be no greater for a turboprop than that for a turbofan if the same level of technology is used. This leaves the cost of the propeller and gearbox, which must be reduced to the level of the fan and reverser in order for the turboprop maintenance costs to be comparable with the turbofan.

The cost drivers and design features of the propeller and gearbox from the 501-D13/54H60 system were examined in the study to project maintainability improvements that could reasonably be expected from a new design for the 1990's. The results of that analysis are summarized in figure 13. The unburdened costs for the 1960-era turboprop (501-D13/54H60) propeller and gearbox scaled to the advanced turboprop mission and size total \$4.58 as shown in the left bar. These same costs could be reduced to \$0.73 in the advanced design by incorporating design features that improve maintainability.

The most significant of these is the elimination of scheduled removals through improved fault isolation and diagnostics. This alone accounted for over 60 percent of the maintenance cost reduction for the propeller and gearbox. The use of modularity is another maintainability feature, common to both the

advanced propeller and gearbox, which was lacking in the 1960-era turboprop. This allows repairs to be made on small equipment packages without disturbing the rest of the engine. Using a simpler design with fewer parts and a more reliable heater accounts for the remaining maintenance cost improvements for the advanced propeller.

Other maintainability features of the advanced gearbox design include using longer life bearings and the removal or simplification of accessories. The engine accessories were removed from the gearbox and installed on the engine core, as is the case for a turbofan; and the aircraft accessories were assumed to be aircraft mounted and their multiple drives simplified to a single shaft. With this arrangement, accessory failures will not require removal of the gearbox as was the case in the 1960-era turboprops.

Since the maintenance costs determined for the advanced turboprop are only estimates, which could prove to be higher in actual practice, the effect of doubling the propeller and gearbox maintenance costs on direct operating costs was evaluated using data from the Lockheed and Boeing RECAT studies (refs. 11 and 15). As shown in figure 14, the effect is small compared with the advantage the turboprop system has over the turbofan.

ADVANCED TURBOPROP AIRCRAFT STUDIES

To evaluate the advanced turboprop's overall impact on complete aircraft configurations, a number of design studies have been completed. Results from three of these studies (refs. 9 to 15) are shown in figures 15 and 16. In figure 15, fuel savings of turboprop (or prop-fan) aircraft are shown relative to turbofan aircraft. Because of different study aircraft configuration assumptions, the prop-fan aircraft fuel savings range from 8 to 28 percent for a 1852-km (1000-n.mi.) stage length. In all cases the increased efficiency of the prop-fan at lower altitudes and speeds results in greater fuel savings at shorter stage lengths. This is one reason why advanced turboprops look particularly attractive for the short- and medium-range flight markets currently being served by the DC-9, B-737, and B-727 aircraft.

The largest fuel saving is for the prop-fan derivative DC9-30 (refs. 12 and 13). The fuel saving is larger than that obtained in the other two studies because the comparison is with the current DC9-30 low-bypass-ratio JT8D turbofan engines. The Douglas study examined two levels of prop-fan performance. One assumed an eight-bladed prop-fan with a rotational tip speed of 219.5 m/sec (720 ft/sec) (corresponding to the Lockheed Electra) and current technology turboshaft engine performance, which would result in a propeller efficiency of 0.73 and an installed cruise thrust specific fuel consumption (TSFC) of 0.0738 kg/hr/N (0.65 lb/lb/hr). The other also assumed an eight bladed prop-fan but with a 243.8 m/sec (800-ft/sec) tip speed and turboshaft engine performance corresponding to the STS-476, a Pratt & Whitney turboshaft engine based on the JT10D engine core, which would result in a propeller efficiency of 0.80 and an installed TSFC of 0.0602 kg/hr/N (0.53 lb/lb/hr). Depending on the assumed propulsion system efficiency, the derivative prop-fan uses 27 to 33 percent less fuel than the DC9-30 at its average operational stage length of 537 km (290 n.

mi.). For the same takeoff gross weight and a passenger load factor of 58 percent, this fuel saving translates into a maximum range improvement of 41 to 73 percent, depending on the propulsion system efficiency assumed.

Admittedly, the fuel saving shown for the prop-fan derivative is higher because the comparison is with an older technology, low-bypass-ratio turbofan rather than a comparable technology turbofan. However, the prop-fan derivative does not include the application of any of the other advanced aerodynamics, structures, or active controls technologies that can improve the efficiency still further. Also, the low-bypass-ratio engines are the ones that are currently being used and sold in large quantities on this airplane type.

In the Lockheed design study (refs. 9 to 11), both the prop-fan and the turbofan were developed using 1985 technology. The resulting fuel saving for the prop-fan aircraft was 20.4 percent for a typical in-service stage length of 880 km (475 n. mi.) and a 58 percent passenger load factor.

The fuel saving for the Boeing prop-fan aircraft compared with an equivalent technology turbofan (refs. 14 and 15) were more modest, amounting to 13.5 percent for the wing-mounted configuration at a 926-km (500-n. mi.) stage length and 13 percent for the aft-mounted configuration. This smaller fuel saving reflects the Boeing study assumptions of a prop-fan noise level in cruise 10 dB higher than the long-range noise goal suggested by Hamilton Standard (the higher noise level results in a larger acoustic treatment weight penalty) and an increase in drag due to the effect of the propeller slipstream on the wing aerodynamics. These two critical technology areas were discussed under Propeller Noise and Fuselage Attenuation and Airframe-Propulsion System Integration sections.

The direction operating cost (DOC) savings identified in these studies (fig. 16) reflect the differences identified in the fuel saving comparisons. The largest DOC saving was obtained for the DC9-30 prop-fan derivative, even at the lower propulsion system efficiency with a TSFC of 0.0738 kg/hr/N (0.65 lb/lb/hr). The DOC saving for this aircraft at a stage length of 537 km (290 n. mi.) was 5.5 percent for fuel at 7.92¢/liter (30¢/gal) and 9.9 percent for fuel at 15.85¢/liter (60¢/gal). The Lockheed prop-fan aircraft obtained a DOC saving for a stage length of 880 km (475 n. mi.) of 5.9 percent for fuel at 7.92¢/liter (30¢/gal) and 8.5 percent for 15.85¢/liter (60¢/gal) fuel. For the Boeing wing-mounted prop-fan, the DOC saving for a 963-km (520-n. mi.) stage length was 4.3 percent with 7.92¢/liter (30¢/gal) fuel and 6.5 percent with 15.85¢/liter (60¢/gal) fuel. The variation with stage length in the DOC savings reflects the trade between the fuel savings percentage decreasing with increasing stage length while fuel cost, as a fraction of DOC, increases.

The results of these 1976 design studies indicated a potential fuel saving of 10 to 20 percent for a wing-mounted prop-fan-powered aircraft relative to a comparable technology turbofan for the same mission cruising at Mach 0.8. This corresponds to a fuel saving of 20 to 40 percent relative to current turbofan aircraft, depending on the current aircraft against which the comparison is made. Accounting for all the design differences between the prop-fan and turbofan-powered aircraft, these fuel savings would result in a

saving in direct operating cost ranging from 3 to 6 percent with 7.92¢/liter (30¢/gal) fuel to 5 to 10 percent with 15.85¢/liter (60¢/gal) fuel.

Lockheed has completed a follow-on study to their original RECAT study. This study was performed to further assess the advantages of a turboprop-powered aircraft for the commercial air transportation system. The advantages of the turboprop aircraft were assessed by comparing them with an equivalent turbofan aircraft. Revised prop-fan aerodynamic and acoustic characteristics were used. The revised data supplied by Hamilton Standard reflected the results of the wind-tunnel tests of an eight-bladed propeller model and included their predictions for a 10-bladed prop-fan. The revised data show an increase in propeller net efficiency of 1.7 percent and an increase in propeller noise during Mach 0.8 cruise of 8 dB for the eight-bladed propeller tip speed of 243.8 m/sec (800 ft/sec). The propeller design trade-offs considered included variations in propeller tip speed, power blading, and number of blades. Fuselage wall-treatment-design assumptions and methods were revised. The treatment now covers the entire circumference of the cabin rather than just the sidewalls. Total treatment length is divided into five segments. Segment length and weight varies with propeller diameter, tip clearance, external sound pressure level and directivity. Also, minimum inner and outer wall weight structural design constraints were imposed for each of the five treatment segments. Besides the original mission calling for Mach 0.8 cruise and a range of 2780 km (1500 n. mi.) two alternative mission were considered: Mach 0.8 cruise with a range of 3700 km (2000 n. mi.) and Mach 0.75 cruise with a range of 2780 km (1500 n. mi.). Comparisons of turboprop and turbofan aircraft were made using alternative and advanced engine technology levels.

The block fuel results are shown in figure 17. The block fuel used by a reference turbofan aircraft for the Mach 0.8 (1500 n. mi.) mission is represented by the bottom bar. Using either of two comparable technology turboprop aircraft, the block fuel savings is 18 percent. When cruise speed is lowered from Mach 0.8 to Mach 0.75, the turboprop block fuel saving becomes 21 percent, which value reflects the higher propulsive efficiency of the turboprop at Mach 0.75. The top two bars show block fuel requirements for a 1990 IOC aircraft. The aircraft are powered by turboprop and turbofan engines having 1985 technology (refs. 4 and 5). For these higher technology engines, the turboprop block fuel savings is 17 percent.

In figure 18 comparisons of turboprop and turbofan aircraft are made in terms of direct operating cost. The PWA turboprop has an 8 percent lower DOC than the turbofan, and the DDA, 10 percent. This additional 2 percent decrease in DOC is due to a significant decrease in installed propulsion system weight. The middle two bars indicate a 10 percent DOC advantage for the turboprop aircraft at Mach 0.75. The top two bars show a comparison for 1990 IOC aircraft. The turboprop DOC saving of 8 percent is the same as for the 1985 IOC aircraft.

SUMMARY OF RESULTS

Before NASA began the Advanced Turboprop Program in October 1977 as the sixth major element in its Aircraft Energy Efficiency Program, NASA supported

some wind tunnel aerodynamic and acoustic tests of propeller models, an experimental wind tunnel program on turboprop-airframe interactions, a study of turboprop maintenance and reliability, and several studies of turboprop-powered commercial transports. These efforts have yielded some encouraging results.

At this time, three highly loaded Mach 0.8 propellers have been built and tested. One of these propellers (SR-1M) was 80 percent efficient when tested at Mach 0.8 and 70 percent of design loading. When tested at Mach 0.7, propeller efficiency was 82 percent at design loading and 85 percent at 70 percent of design loading. Early experimental results on turboprop-airframe interactions indicate that installation drag need not be large. Moreover, designing the wing to accommodate swirl in the propeller slipstream has the potential of reducing installation drag. The study of turboprop system reliability and maintenance cost concluded that an advanced turboprop and an advanced turbofan, using similar cores, would have very competitive maintenance costs. A recent study to assess the potential of turboprop-powered aircraft relative to turbofan-powered aircraft confirms the earlier study results. With 15.85¢/liter (60¢/gal) fuel, the DOC advantage of the turboprop aircraft is about 10 percent. The fuel saving for medium-range turboprop-powered aircraft is 21 percent for Mach 0.75 aircraft and 17 percent for Mach 0.8 aircraft.

REFERENCES

1. Klineberg, J. M.: Technology for Aircraft Energy Efficiency. Presented at the American Society of Civil Engineers, International Air Transportation Conference, (Wash., D.C.), Apr. 4-6, 1977.
2. Neitzel, R. E.; Hirschcron, R.; and Johnston, R. P.: Study of Turbofan Engines Designed for Low Energy Consumption. (R76AEG432, General Electric Co., NASA Contract NAS3-19201.) NASA CR-135053, 1976.
3. Neitzel, R. E.; Hirschcron, R.; and Johnston, R. P.: Study of Unconventional Aircraft Engines Designed for Low Energy Consumption. (R76AEG597, General Electric Co.; NASA Contract NAS3-19519.) NASA CR-135136, 1976.
4. Gray, D. E.: Study of Turbofan Engines designed for Low Energy Consumption. (PWA-5318, Pratt & Whitney Aircraft; NASA Contract NAS3-19132.) NASA CR-135002, 1976.
5. Gray, D. E.: Study of Unconventional Aircraft Engines Designed for Low Energy Consumption. (PWA-5434, Pratt & Whitney Aircraft; NASA Contract NAS3-19465.) NASA CR-135065, 1976.
6. Dugan, J. F.; Bencze, D. P.; and Williams, L. J.: Advanced Turboprop Technology Development. AIAA Paper 77-1223, Aug. 1977.
7. Rohrbach, C.: A Report on the Aerodynamic Design and Wind Tunnel Test of a Prop-Fan Model. AIAA Paper 76-667, July 1976.
8. Mikkelson, D. C., et al.: Design and Performance of Energy Efficient Propellers for Mach 0.8 Cruise. SAE Paper No. 770458, Mar. 1977.
9. Foss, R. L.; and Hopkins, J. P.: Fuel Conservation Potential for the Use of Turboprop Powerplanes. SAE Paper 760537, May 1976.
10. Hopkins, J. P.; and Wharton, H. E.: Study of the Cost/Benefit Tradeoffs for Reducing the Energy Consumption of the Commercial Air Transportation System. (LR-27769-1, Lockheed-California Co.; NASA Contract NAS2-8612.) NASA CR-137927, 1976.
11. Hopkins, J. P.: Study of the Cost/Benefit Tradeoffs for Reducing the Energy Consumption of the Commercial Air Transportation System. (LR-27769-2, Lockheed-California Co.; NASA Contract NAS2-8612.) NASA CR-137926, 1976.
12. Stern, J. A.: Aircraft Propulsion - A Key to Fuel Conservation: An Aircraft Manufacturer's View. SAE Paper 760538, May 1976.

13. Kraus, E. F.: Cost/Benefit Tradeoffs for Reducing the Energy Consumption of Commercial Air Transportation System. Vol. I: Technical Analysis. (MDC-J7340-Vol.-1, Douglas Aircraft Co., Inc.; NASA Contract NAS2-8618.) NASA CR-137923, 1976. Van Abkoude, J. C.: Cost/Benefit Tradeoffs for Reducing the Energy Consumption of Commercial Air Transportation System. Vol. II: Market and Economic Analyses. (MDC-J7340-Vol.-2, Douglas Aircraft Co., Inc.; NASA Contract NAS2-8618.) NASA CR-137925, 1976.
14. Energy Consumption Characteristics of Transports Using the Prop-Fan Concept: Summary (D6-75780, Boeing Commercial Airplane Co.; NASA Contract NAS2-9104.) NASA CR-137938, 1976.
15. Energy Consumption Characteristics of Transports Using the Prop-Fan Concept: Final Report. (D6-75780, Boeing Commercial Airplane Co.; NASA Contract NAS2-9104.) NASA CR-137937, 1976.
16. Shollenberger, C. A.: Three-Dimensional Wing/Jet Interaction Analysis Including Jet Distortion Influences. J. Aircraft, vol. 12, no. 9, Sep. 1976, pp. 706-713.
17. Rubbert, P. E.; and Saaris, G. R.: Review and Evaluation of a Three-Dimensional Lifting Potential Flow Computational Method for Arbitrary Configurations. AIAA Paper 72-188, Jan 1972.
18. Hess, J. L.: Calculation of Potential Flow About Arbitrary Three-Dimensional Lifting Bodies. MDC-J5679-01, Douglas Aircraft Co., Inc., 1972.
19. Stolp, P. C.; and Baum, J. A.: Advanced Turboprop Propulsion System Reliability and Maintenance Cost. SAE Paper-771009, Presented at the SAE Aerospace Engineering and Manufacturing Meeting, (Los Angeles, Calif.), Nov. 14-17, 1977.

TABLE I. - MEASURED MODEL PROPELLER PERFORMANCE^a

[Advance ratio, J, 3.06; power coefficient, C_p, 1.7.]

Configuration	Blade tip sweep, deg	Design point efficiency, ^b %		Measured efficiency, ^c percent
		Current prediction	Test data	
SR-1	30	78.9	77.1	80.2
SR-1M	30	79.2	77.1	81.7
SR-2	0	76.6	77.0	80.2

^aData taken in the Lewis 8- by 6-foot wind tunnel.

^bMach 0.8; power loading, 310 kW/m² (37.5 hp/ft²); tip speed, 244 m/sec (800 ft/sec).

^cMach 0.7.

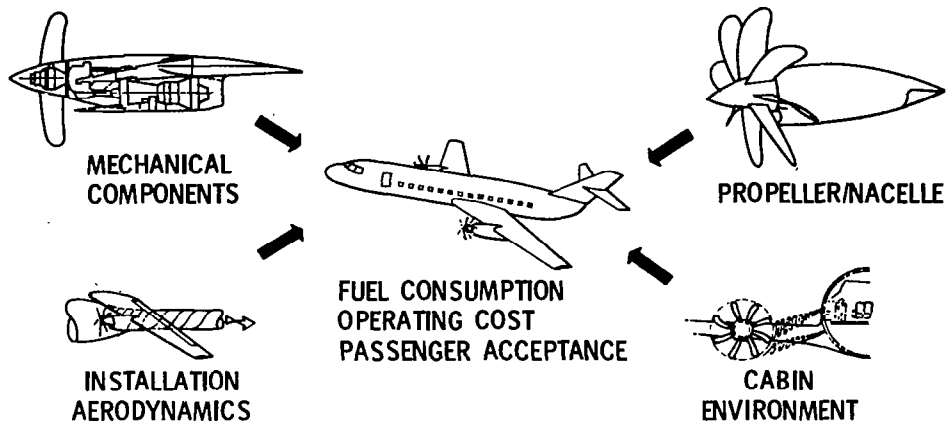


Figure 1.- Major areas of advanced turboprop program.



Figure 2.- Propeller model in Lewis wind tunnel.

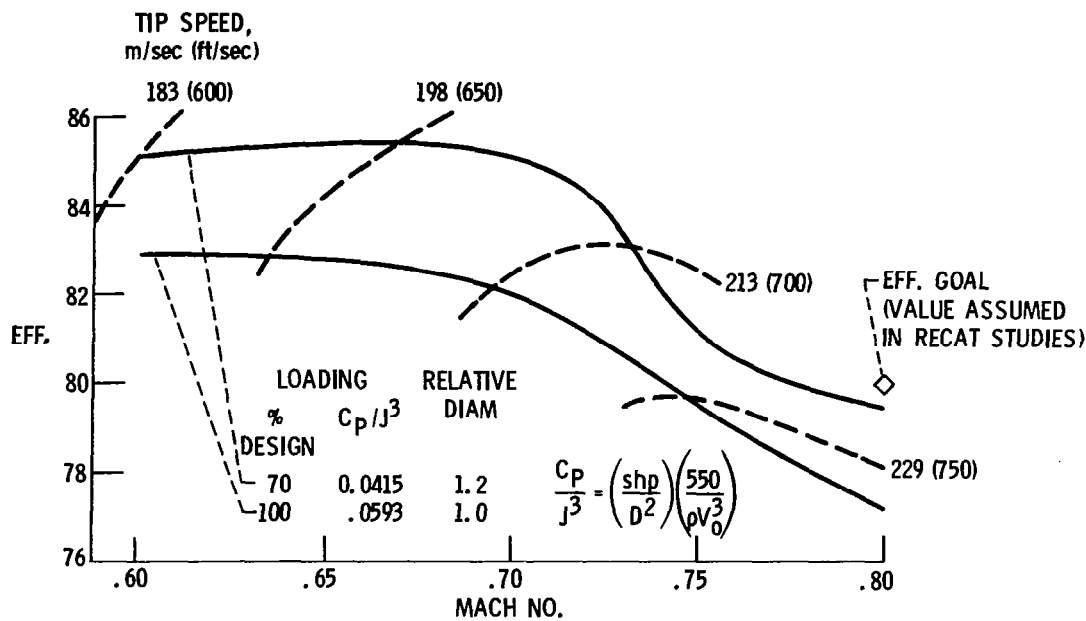


Figure 3.- Effect of cruise Mach number on efficiency. Propeller model SR-1M; data taken in Lewis 8- by 6-ft wind tunnel; blade angle and tip speed varied for maximum life.

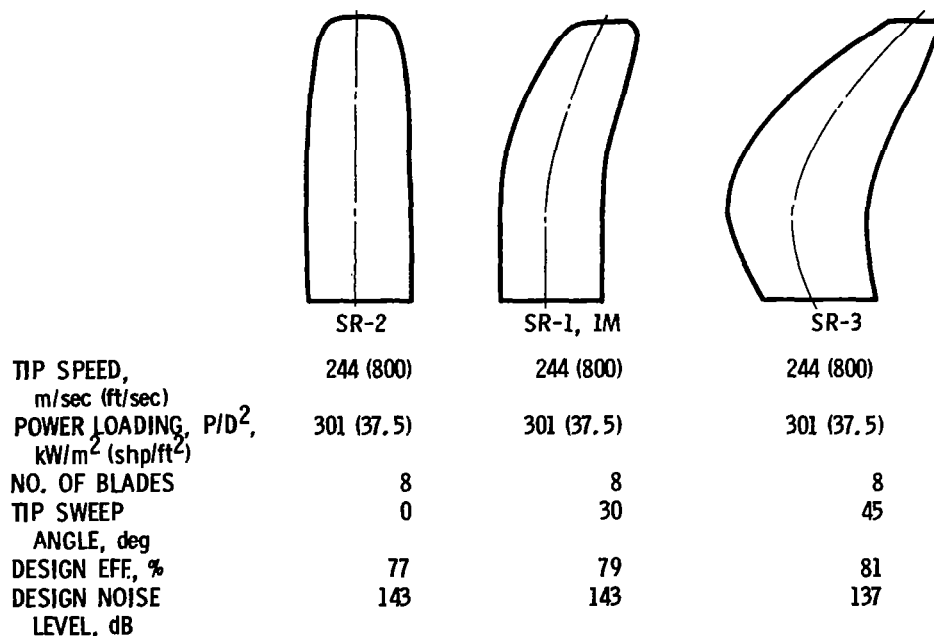


Figure 4.- Comparison of propeller models.

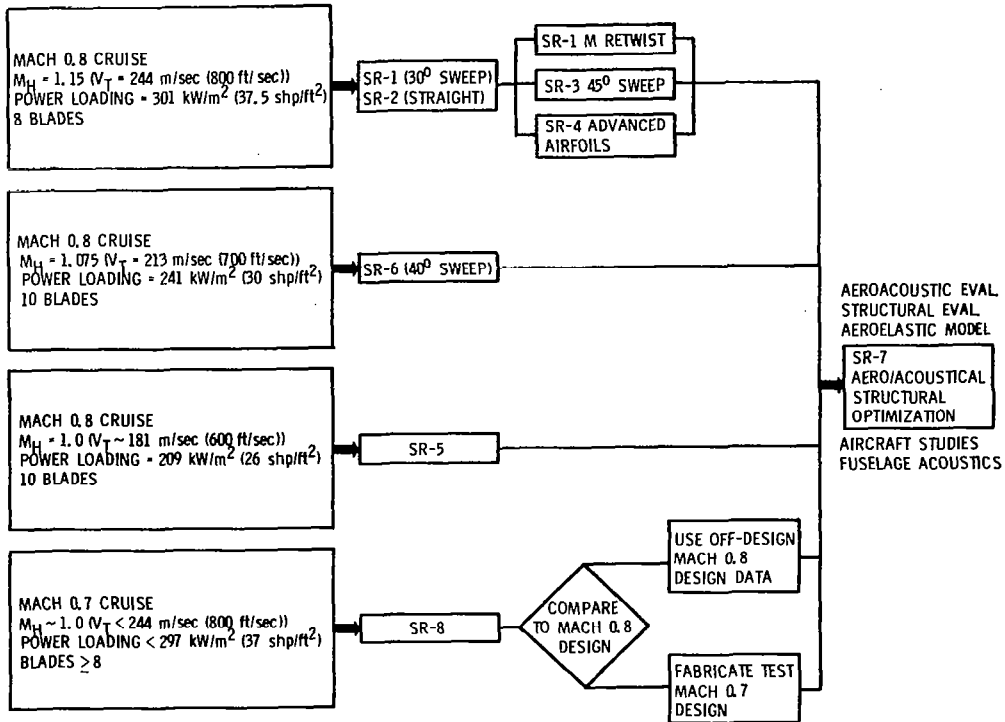


Figure 5.- Current propeller model performance test program.

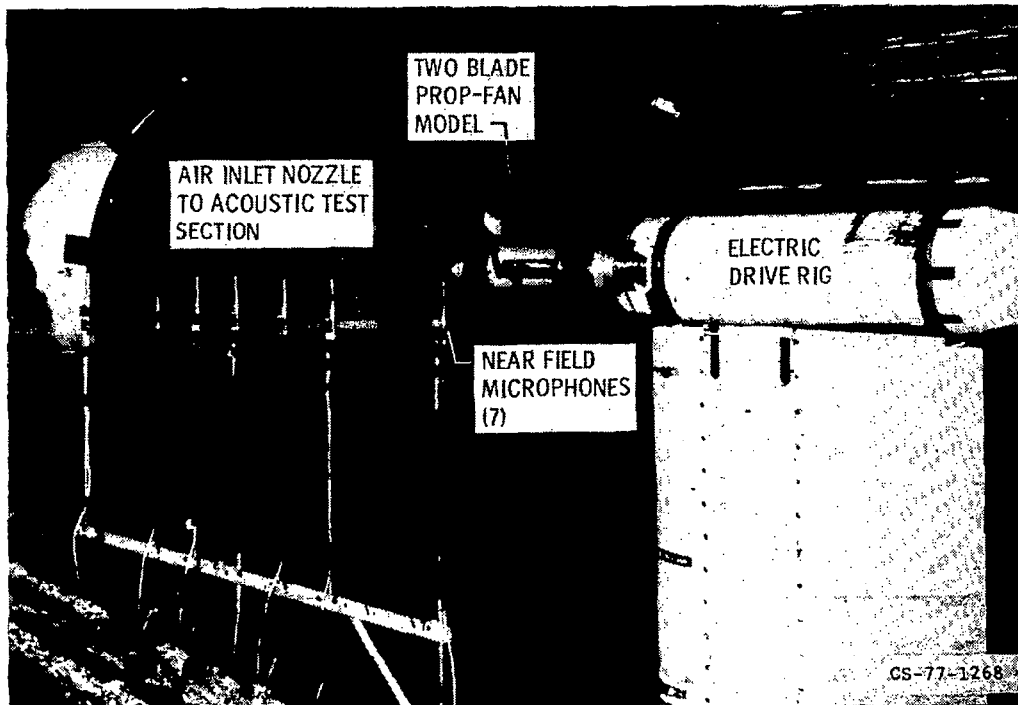


Figure 6.- Propeller model tests in UTRC acoustic research tunnel.

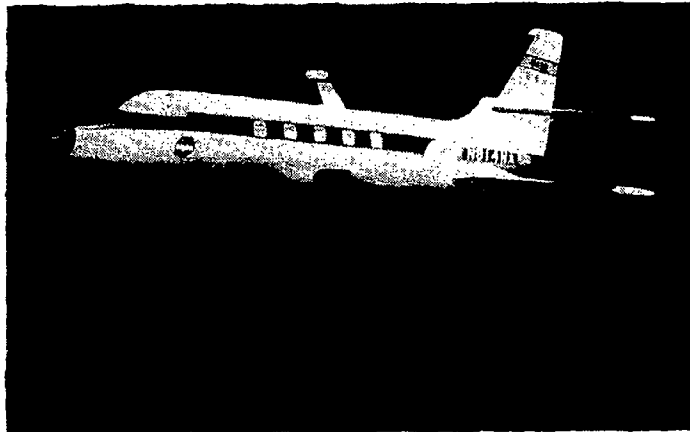


Figure 7.- Depiction of propeller model mounted on aircraft for acoustic tests.

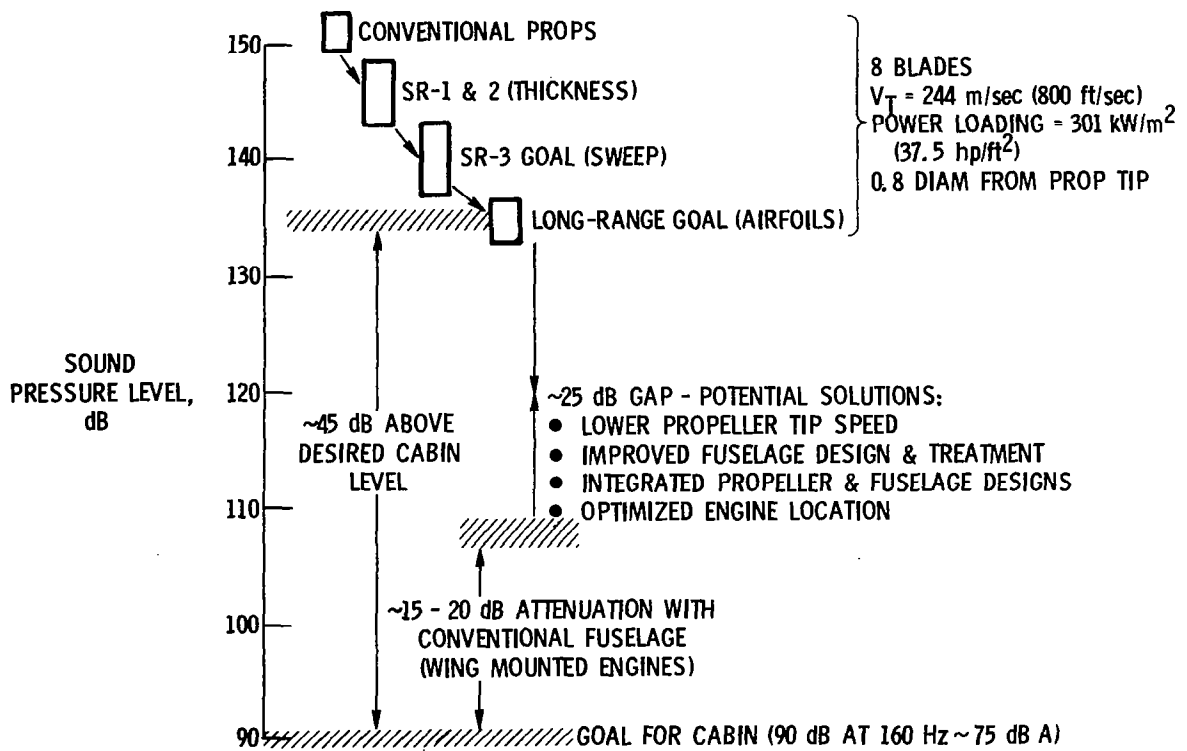
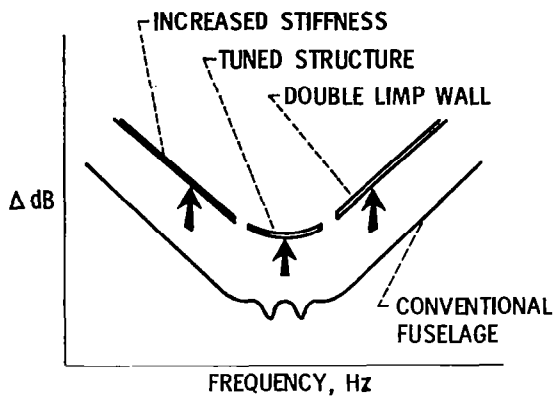
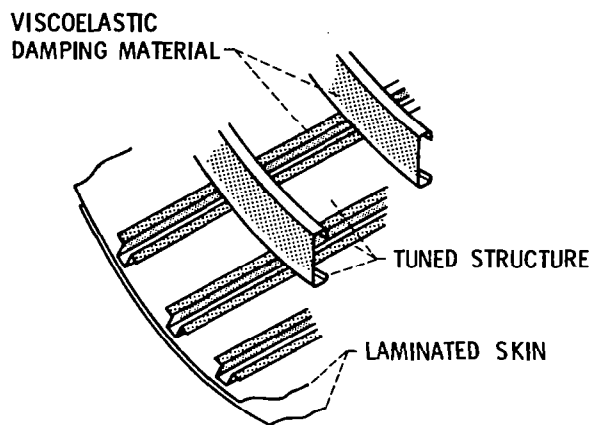


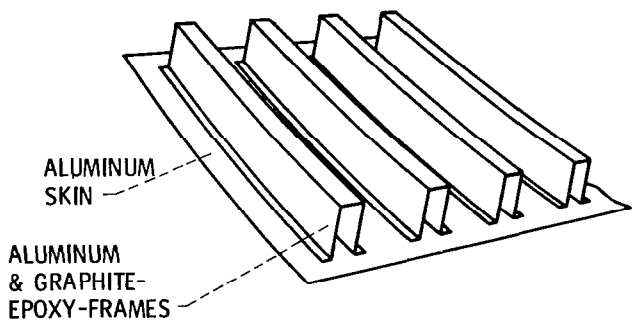
Figure 8.- Propeller and cabin noise. Cruise speed, Mach 0.8; altitude, 10.67 km (35 000 ft).



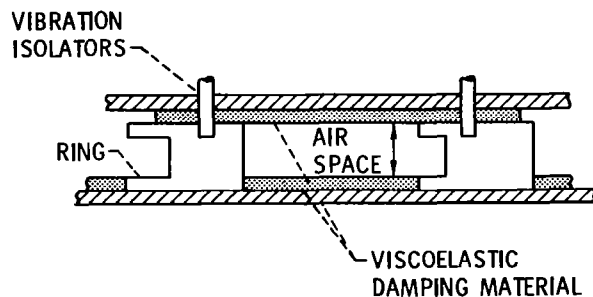
(a) Effect of frequency.



(b) Tuned structure.

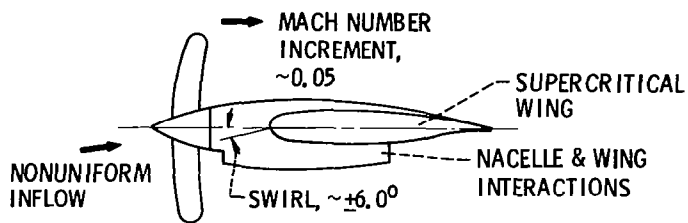


(c) Increased stiffness.



(d) Double limp wall.

Figure 9.- Fuselage structural concepts for propeller noise reduction.



- ASSESS MAGNITUDE OF AERODYNAMIC INTERFERENCE
- UNDERSTAND AERODYNAMIC PHENOMENA
- DEVELOP ANALYTICAL & EXPERIMENTAL DATA BASE
- USE SLIPSTREAM SIMULATOR & POWERED SEMISPAN MODEL

Figure 10.- Airframe-propulsion system integration program.

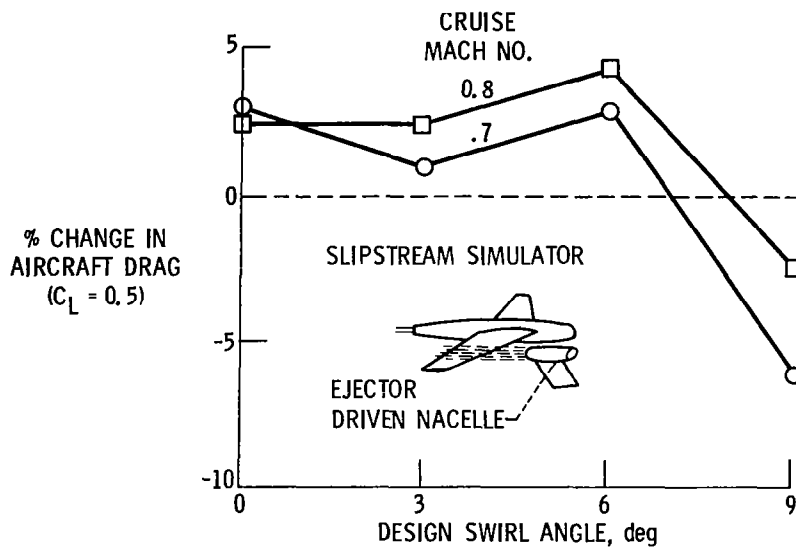


Figure 11.- Effect of simulated slipstream on aircraft cruise drag. Preliminary ARC wind tunnel data. Slipstream Mach number variation, 0.075.

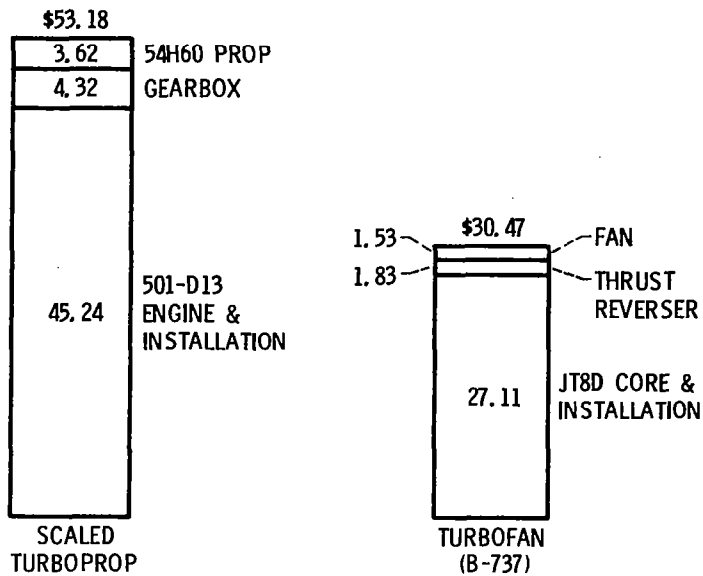


Figure 12.- Comparison of 1960-era turboprop and turbofan maintenance costs. Fully burdened cost in 1976 dollars per flight hour; duty cycle, 1.3 per engine flight hour.

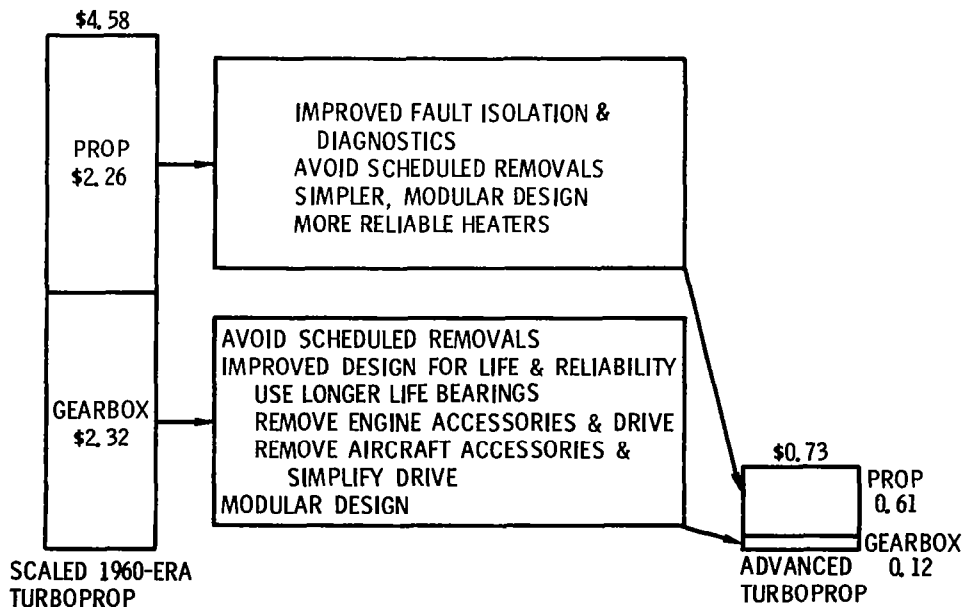


Figure 13.- Maintenance cost reduction for propeller and gearbox. Unburdened costs in 1976 dollars per flight hour; duty cycle, 1.25 per flight hour.

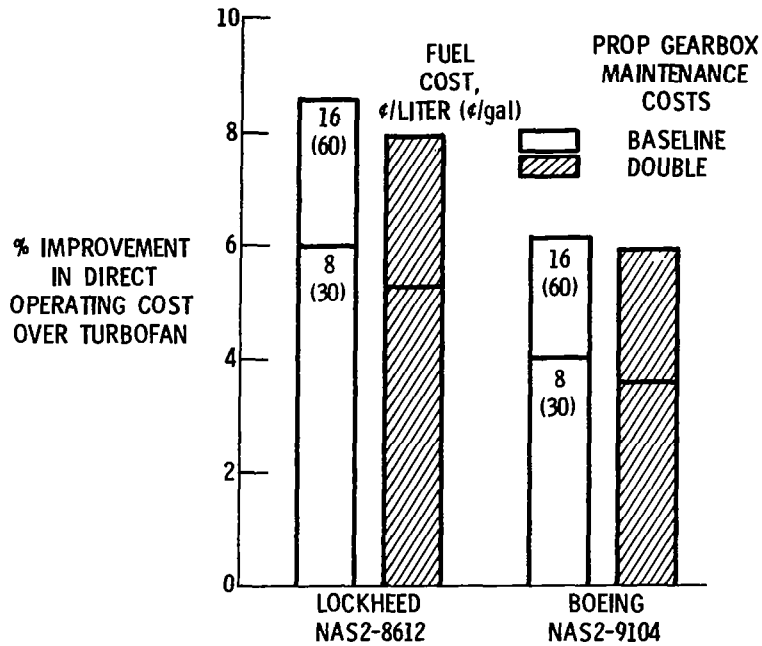


Figure 14.- Direct operating cost sensitivity to propeller and gearbox maintenance costs.

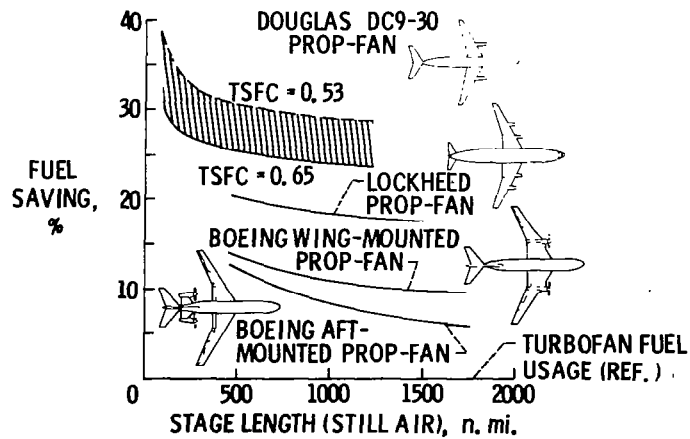


Figure 15.- Turboprop aircraft fuel savings.

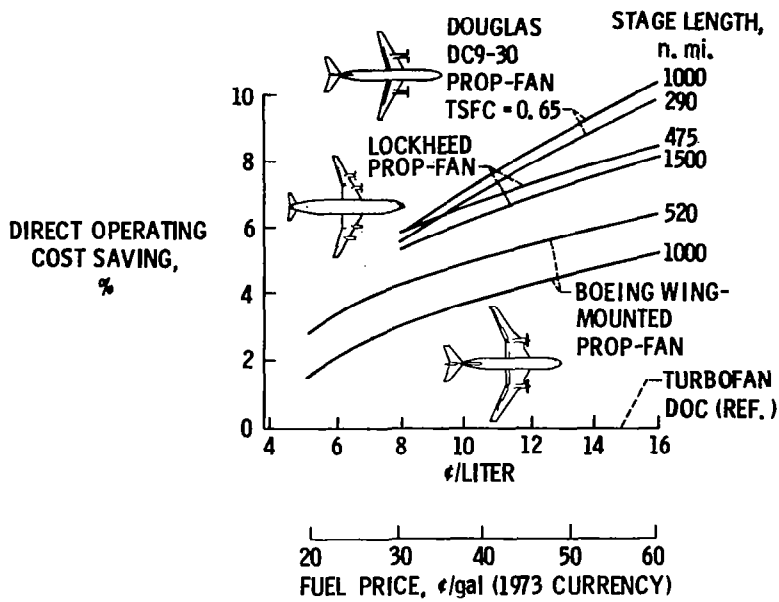


Figure 16.- Turboprop aircraft operating cost savings.

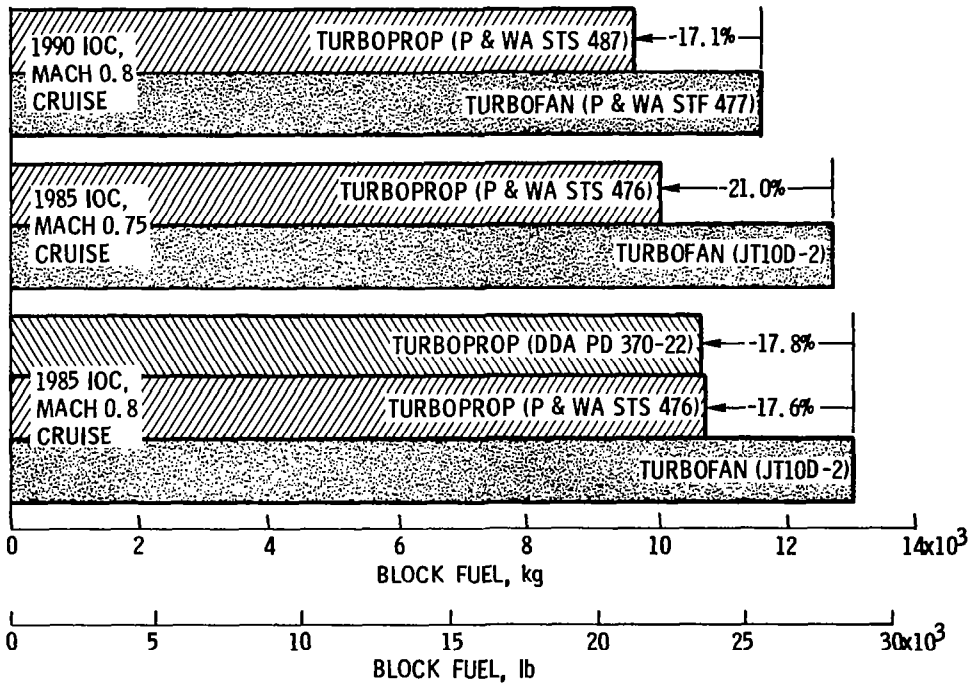


Figure 17.- Effect of aircraft design on block fuel usage. Data from Lockheed RECAT follow-on study (NAS2-8612). Mission Characteristics: Number of passengers, 200; trip distance, 2780 km (1500 n. mi.); load factor, 100 percent. Design characteristics: four wing-mounted engines; eight-bladed propellers (on turboprops).

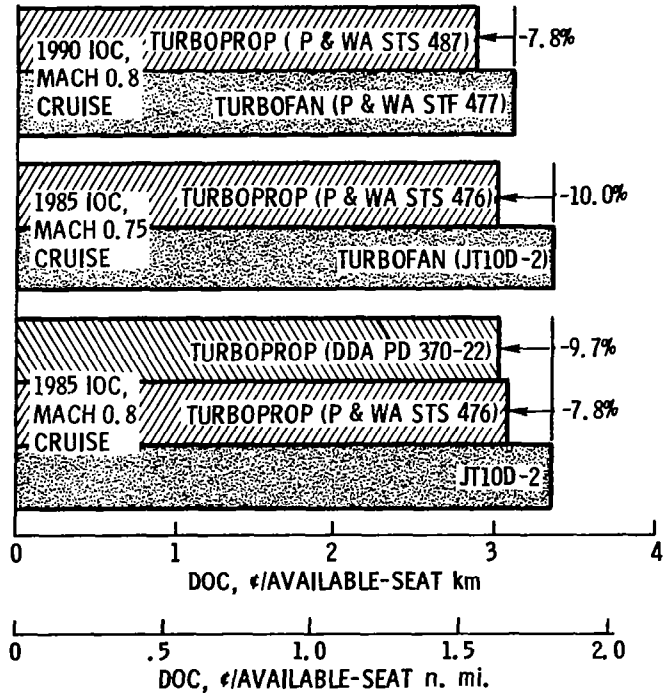


Figure 18.- Effect of aircraft design on direct operating costs. Data from Lockheed RECAT follow-on study (NAS2-8612). Mission characteristics: Number of passengers, 200; trip distance, 2780 km (1500 n. mi.); load factor, 100 percent. Design characteristics: four wing-mounted engines; eight-bladed propellers (on turboprops). Fuel cost, 15.85¢/liter (60¢/gal).